

LORAN-C LATITUDE-LONGITUDE CONVERSION AT SEA : PROGRAMMING CONSIDERATIONS

by James R. McCULLOUGH(*), Barry J. IRWIN(**)
and Robert M. BOWLES(**)

This is an abridged version of a paper, originally presented at the 1982 Wild Goose Association (WGA) Technical Symposium, for which the WGA awarded the "Best Paper Award" to the authors at its twelfth annual convention, Washington, D.C., October 1983. A copy of the original paper will be furnished by the IHB on request.

ABSTRACT

To aid programmers of LORAN-C latitude-longitude conversion, we :

1. Provide reference to the literature.
2. Compare digital "processings-noise" for several arc-length methods.
3. Discuss some practical aspects of overland signal propagation (ASF) modeling for offshore navigation.

Comparisons are made of the precision of arc-length routines as computer precision is reduced. Overland propagation delays (ASF's) are discussed and illustrated with observations from offshore New England. Present practice of LORAN-C error budget modeling is then reviewed with the suggestion that additional terms be considered in future modeling.

INTRODUCTION

LORAN-C is a pulsed, 100-kHz, groundwave, hyperbolic navigation aid with extensive world coverage. Its accuracy is conservatively rated at 1/4 nautical mile (500 m) over a range of about 800 nautical miles. Repeatability (a measure of the resolution and stability of the LORAN observation) is more nearly 20-100 m. The

(*) Woods Hole Oceanographic Institution, Woods Hole, Mass. 02543, USA.

(**) U.S. Geological Survey, Woods Hole, Mass. 02543, USA.

accuracy with which latitude and longitude can be determined can approach this level via calibrated radio propagation models. Such model techniques are currently under study at the United States Coast Guard (USCG) and the Defense Mapping Agency/Hydrographic Topographic Center (DMA).

Until 1981, DMA LORAN error model coefficients and results were classified. Their declassification, together with the recent evolution of microprocessors, has generated renewed interest in LORAN calibration, particularly for harbor navigation and offshore survey applications. For offshore survey work in good LORAN coverage, an order of magnitude improvement in positional accuracy is feasible with no change in present equipment. Technically, the calibration process requires detailed error models and field calibration data. Practically, calibration requires organization, funding, and motivation.

But why calibrate LORAN when world coverage with the Navstar Global Positioning System (GPS) is nearly here? We propose to calibrate and pace. That is, to use GPS now to help calibrate and improve LORAN, and to use LORAN in the future to pace GPS.

This paper presents results of studies conducted by the U.S. Geological Survey at Woods Hole, Mass. In it, we evaluate several arc-length methods, discuss LORAN propagation model parameters, and compare present model predictions with offshore observations. We have included some details that were initially puzzling or not readily available during our learning process; we hope they will be of interest to others. Our intent is to provide a tutorial overview and entry to the literature for readers familiar with basic LORAN technology. Excellent LORAN primers, histories, and reviews include BIGELOW (1965), Canadian Coast Guard Primer (1981), GRANT (1973), HEFLEY (1972), U.S. Coast Guard Handbook (1980), and WESEMAN (1982 b).

BACKGROUND

Overview

The LORAN latitude/longitude conversion process has three parts. It is necessary to find :

- 1) Arc-length (the distance between two points on the Earth ellipsoid);
- 2) Distance to time conversion (the radio travel-time for a given arc-length); and
- 3) Time Difference (TD) to latitude/longitude conversion (the latitude and longitude of a given TD pair having solved for items 1 and 2).

The last step is implemented as an iterative solution or in closed form (COLLINS, 1980; FELL, 1975; RAZIN, 1967; and STUIFBERGEN, 1980). Its somewhat involved processing details are well documented in the literature and are, therefore, not covered here. This paper discusses steps 1 and 2, with emphasis on the distance to time conversion which now represents the largest single error source in LORAN surveying.

Arc-length Methods

Numerous arc-length methods have been developed. Appendix A compares results calculated with the SODANO (1965), COLLINS (1980), LAMBERT (1942), and THOMAS (1970) methods using different computer precision. The SODANO method is the least sensitive to reduced precision. Example code and test problems give distance, forward azimuth, backward azimuth and the RTCM SALT-model travel time. (RTCM in this paper stands for the now defunct Radio Technical Commission for Marine Services, a cooperative government and industrial advisory commission. The present RTCM or Radio Technical Commission for Maritime Services continues the earlier work without direct government affiliation).

The RTCM (1981) method is somewhat harder to program than the original SODANO (1965) method. With the latter, longitude (positive east) can be entered directly and the azimuths require no additional testing when returned with a four-quadrant tangent solution.

Length and Time

Given an arc-length, d , in meters, it is desired to find the LORAN travel-time, t , in microseconds. The technique used by DMA and the USCG is described in the section on propagation below. Their method is reduced to three terms called the primary-phase factor (PF), the secondary-phase factor (SF), and the additional secondary-phase factor (ASF). The total phase Φ_T is :

$$\Phi_T = PF + SF + ASF$$

and

$$t = \frac{\Phi_T}{2\pi f} \times 10^6 \text{ } \mu\text{sec}$$

$$= 5\Phi_T/\pi$$

where $f = 100,000$ Hz is the LORAN center-frequency, and t is the desired propagation time. The travel-time code can be programmed on a pocket calculator, such as the HP-41CV, (i.e. NEWMAN, 1980; and NEWMAN, 1982). The travel-time of the PF (t_{PF}) equals the arc-distance, d , divided by the mean speed, \bar{C} , of LORAN waves in homogeneous air with no earth effects, i.e.,

$$t_{PF} = d/\bar{C}$$

where $\bar{C} = C_0/n$, C_0 equals the speed of light in free-space, and n is a nominal index of refraction of air. The travel time of the SF term (t_{SF}), is found from polynomial approximations of the nominal salt-water conditions tabulated in JOHLER et al. (1956). Finally, the travel time of the ASF term (t_{ASF}), is tabulated by DMA from detailed geographical, geological, theoretical, and observational data. Thus, the total travel-time, t , is :

$$t = t_{PF} + t_{SF} + t_{ASF}$$

The primary and secondary terms are fixed by definitions discussed below. The ASF term is usually relatively small and accounts for the additional travel-time due to planetary boundary conditions other than those of the standard salt-water model used in the SF calculation.

Other conditions related to LORAN chain timing (weather effects, seasons, climate, pulse shape, skywave, noise, etc.) are generally not modeled by DMA but are partially compensated by active steering of the LORAN chain timing.

Fixed Coefficient Model (Present status)

The DMA LORAN propagation model, RTCM (1981), has a fixed structure with fixed coefficients. It provides a much needed community-wide standard of sufficient accuracy for most needs. It makes a one-time adjustment to local conditions at the time of calibration. Obviously, a simplified model with fixed coefficients cannot be optimal for all places and conditions.

Unfortunately, the model assumptions and travel-time sensitivity of each of the nominal values are not readily available. We have indicated a few error estimates in parts per million (ppm) below. (The ppm values are equivalent to 1 m at 10^6 m or about 540 nautical miles, a reasonable outer working range for good coverage. Some errors are not linearly range-dependent, so the ppm values are only intended to indicate the relative importance of parametric variations.)

Variable Coefficient Models

Propagation models which adapt their coefficients to space-time variations and which model many error terms could be applied to LORAN as they have been applied in Transit satellite and GPS navigation. Although such models lose the attractive features of simplicity, they should allow greater accuracy where required. The information rate required for adaptive LORAN models is low, a few bits per hour. This input might come from special seasonal charts, local weather observations, or fixed-site "Local Area Monitors" (LAM's) functioning like the present "System Area Monitors" (SAM's) but with local feedback. Ultimately, the LAM correction vectors might be transmitted with the LORAN message. Harbor navigation research is currently studying LAM or differential LORAN techniques.

Calibration and Control

The latitude and longitude of the transmitters and SAM's are determined from Transit satellite surveys and converted to WGS-72 coordinates. An atomic "Hot Clock" is then flown between Master and Secondary transmitters and used to directly measure the Emission Delay (ED), the time between the Master and Secondary transmissions. While the ED calibration is being made, the time difference (TD) at the SAM is also measured. This Controlling Standard Time Difference (CSTD) is used for routine control of the Secondary's transmission time relative to that of the Master. The latitudes, longitudes, nominal ED's and CSTD's are published (USCG, 1981) and updated periodically. Corrections to the Secondary's timing, the Local Phase Adjustments (LPA's), are made in 20-nsec steps at 7.5-minute intervals. Timing control at the Secondary is such that only about one

LPA per hour is required under normal conditions. Note that the LPA's attempt to maintain constant CSTD, *not* constant ED. The LPA's primarily track propagation variation; clock and transmitter changes are generally smaller and of longer period.

Steering the secondary in order to hold a constant TD at the SAM has several important consequences. First and foremost, it works rather well. Variations in the primary service area of 9960, for example, are typically less than 100 nsec (USCG, 1982). Second, the ED is not constant. Uniform changes in propagation speed are fully compensated along the locus of positions that are roughly the same land-length difference from the transmitters as the SAM. Third, stations at increasing distance from this SAM locus show increasing errors. Finally, the non-uniform components of propagation variations caused by local weather patterns, etc., are reflected in a complex manner throughout the service area. The USCG has recently established TD monitors at about 20 sites in the United States to routinely observe such variation. These observations (USCG, 1982) will hopefully lead to practical error models and/or real-time corrections for propagation variations. The SAM errors are the next largest term in the LORAN error budget after the ASF's.

Pulse Geometry

The ground-wave component of the hemispherically expanding LORAN pulse shell can be visualized as a cylindrical ring spreading over the curved earth. The ring has a width of about 50 km, a height of only a few kilometers, and grows at nearly the speed of light to a useful diameter of 3000 km or more while its strength decreases rapidly with distance. We are interested in one particular electric field surface near the outer edge of the ring, the surface associated with the zero-crossing of the end of the third cycle. Its noise-limited width is only about 3-30 m.

The pulse phase-surfaces tilt slightly forward and increase in signal strength with altitude over land. The forward tilt produces a small radial component of the electric field in the ground which acts as a "lossy" dielectric, slowing and attenuating the wave. As the pulse moves out to sea, the surface losses are abruptly reduced by several orders of magnitude, exciting higher order propagation modes and allowing energy from modes aloft to advance the near-surface wave-front. The rapid advance at the surface actually reduces the accumulating phase lag and is thus called a "phase recovery." This effect is seen in the model predictions of Figure 1. The correction (bottom curve) grows rapidly at first and drops abruptly at the first conductivity boundary near the Hudson River. Before this recovery is complete, the error curve drops abruptly again at the shore at Weekapaug, R.I. The first phase recovery is undoubtedly a model artifact, but the second is quite real, as will be illustrated by the observational data in Figure 7 below.

A similar sky wave arrives later than the ground wave via the ionosphere. The sky-wave delay and relative amplitude increase at night when the ionosphere is higher. By sampling early in the pulse at the end of the third cycle, most of the sky-wave interference is removed even when the sky wave is considerably stronger than the earlier arriving ground wave.

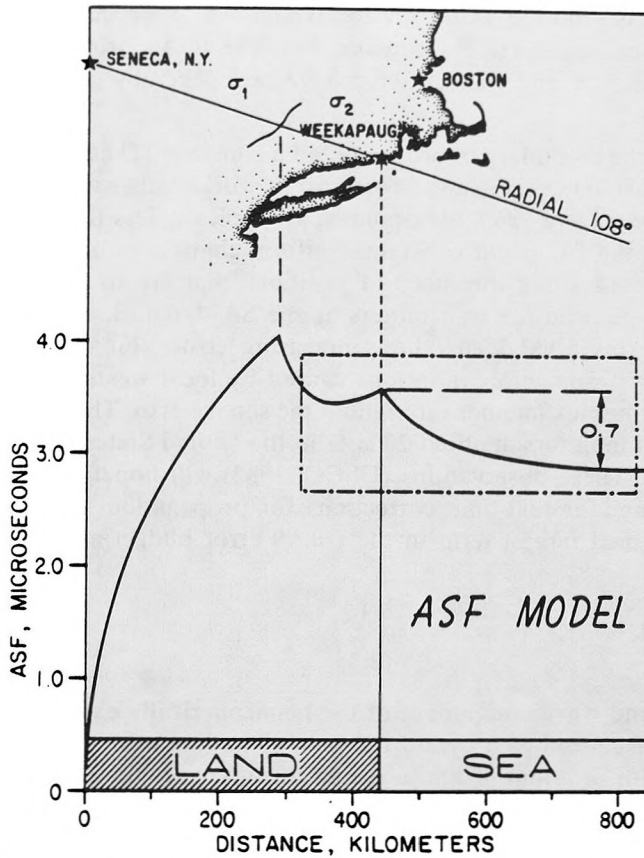


FIG. 1. — Range ASF model predictions along radial 108° from the 9960-Master at Seneca, NY. Phase-recovery is seen in the model at the conductivity changes near the Hudson River and at the shore near Weekapaug, RI.

PROPAGATION PREDICTION

The Van der POL-BREMMER Propagation Method

The LORAN propagation method used by DMA and the USCG is described by Van der POL and BREMMER (1937, 1938 and 1939) and BREMMER (1949 and 1958). It has been numerically tabulated by JOHLER et al. (1956), BRUNAVS (1976 and 1977), and BRUNAVS and WELLS (1971 a). The model assumes a smooth, spherical earth of finite conductivity, dielectric constant, and permeability with an electric point source near the earth's surface. Both the model and its numeric evaluation presented formidable problems for nearly half a century. It is now one of many models available (HUFFORD, 1952; JOHLER, 1970; SAMADDAR, 1979; and WAIT, 1981). The Van der Pol-Bremmer method assumes continuous wave (CW) propagation at a single frequency with no skywave interference. The phase of the far field wave, Φ , is

$$\Phi = K_1 d + \Phi_c \quad (1)$$

where the wave number K_1 is

$$K_1 = \frac{\omega n}{C_0} = \frac{2\pi}{\lambda}$$

and

$$\omega = 2\pi f \text{ and } \lambda = \text{wavelength} = 3 \text{ km}$$

The first term ($K_1 d$) accounts for propagation through the air and Φ_c treats the effects of refraction, diffraction, modal propagation, boundary conditions, and initial conditions as seen in the far field.

$$\Phi_c = \arg \left[\sum_{\sigma=0}^{\infty} \frac{1}{2\tau_s^{-1}/\delta^2} \exp \left\{ i \left[(K_1 a)^{1/3} \tau_s \alpha^{2/3} \frac{d}{a} + \frac{\alpha d}{2a} + \frac{\pi}{4} \right] \right\} \right] \quad (2)$$

and the time t_c associated with Φ_c is found from

$$t_c = \frac{\Phi_c}{\omega} \times 10^6 \text{ } \mu\text{sec} \quad (3)$$

Where a = earth radius, d = distance from the transmitter; α and δ are discussed below. The factors τ_s are solutions to Riccati's differential equation (HOWE, 1960; and JOHLER et al., 1959),

$$\frac{d\delta}{d\tau_s} - 2\delta^2 \tau_s + 1 = 0 \quad (4)$$

where δ is a frequency dependent conductivity and permittivity parameter for a vertical electric dipole,

$$\delta = \frac{i (K_2/K_1)^2 \alpha^{1/3}}{(K_1 a)^{1/3} ((K_2/K_1)^2 - 1)^{1/2}} \quad (5)$$

where the earth wave number K_2 is

$$K_2 = \frac{\omega}{C_0} \left[\epsilon_2 + i \frac{\sigma \mu_0 C_0^2}{\omega} \right]^{1/2} \quad (6)$$

Given d , the coefficients needed to solve for Φ_c from equations 2-6 are : w , μ_0 , C_0 , a , n , α , ϵ_2 and σ . As the first four are known, Φ_c is a function of the atmospheric parameters n and α and the earth effective impedance factors ϵ_2 and σ , i.e. :

$$\Phi_c = f(n, \alpha, \epsilon_2, \sigma) \quad (7)$$

Note that Φ and therefore the scale and, to some extent, the rotation of the LORAN grid is a function of n , α , ϵ_2 , and σ . Thus the selection of the air parameters n and α is critical and should be made independently of the earth boundary conditions treated by τ_s . From equation (1) it is seen that the primary factor time $t_{PF} = \Phi_c/w$ is

$$t_{PF} = K_1 d / \omega = nd / C_0;$$

it is not frequency dependent but the secondary factor time, t_{SF} , is.

BRUNAVS (1977) gives two polynomial approximations for t_c (equation 3) and calculates their errors compared with direct solutions. SAMADDAR (1979, 1980) reviews the theory treated extensively in WATSON (1918), Van der POL and BREMMER (1937, 1938, 1939), BREMMER (1949, 1958), JOHLER et al. (1956), and JOHLER (1962). WAIT (1964, 1981), and FOCK (1965) provide modern perspective and entry to the extensive literature on this and other model approaches. The older Van der

POL-BREMMER method is outlined here because of its historic significance and its use by DMA and the USCG. With modern computers, it offers little advantage over the more flexible and direct numeric integration methods.

Sea Water Effects

Fortunately, sea-water variations have little effect on LORAN propagation. The skin depth (depth at which the signal is attenuated by $1/e$, TERMAN, 1943) of the waves is about 75 cm. Although the temperature and salinity of sea water vary

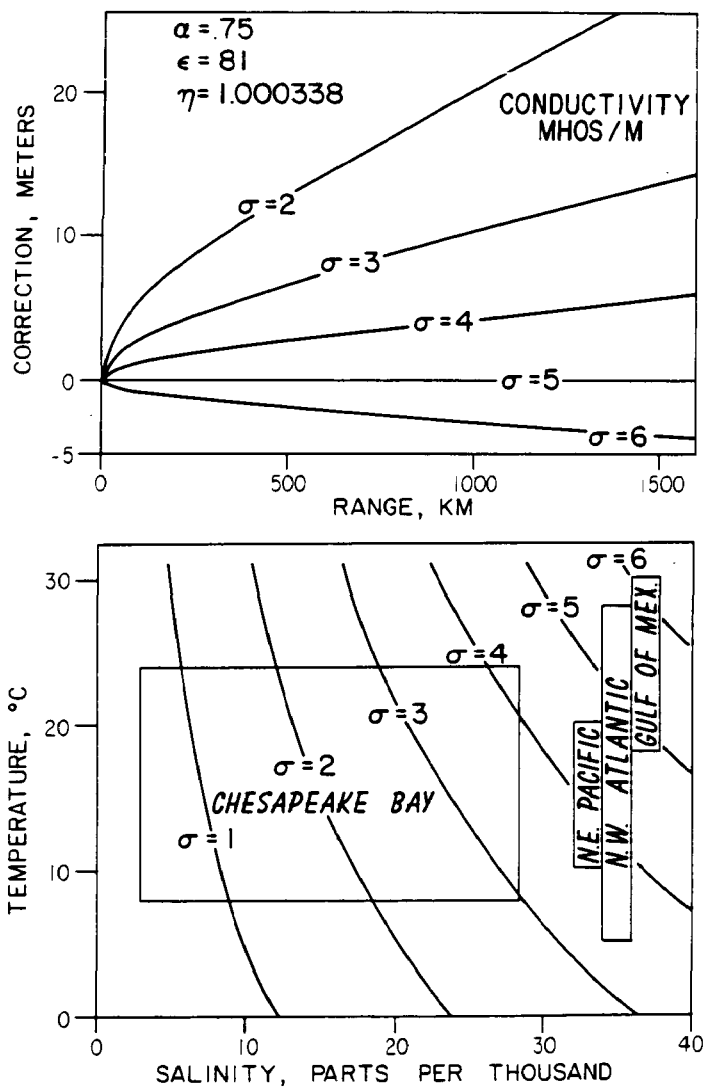


FIG. 2. — Relationship between salinity, temperature and conductivity (bottom) for sample near-surface ocean conditions (blocks at bottom). The range of conductivity shown can then be translated (top) to range errors in meters relative to the "standard" conductivity of 5 mhos/meter.

considerably near the ocean surface, associated conductivity changes produce only small propagation variations.

To illustrate this, the lower half of Figure 2 shows the variation of conductivity with temperature and salinity, together with broad outlines of various near-surface water types. The upper half of the figure gives the error in meters relative to $\sigma = 5$ as a function of range. As seen, errors of only a few meters or so in the range estimates are expected from this source. The effect of ocean surface waves on LORAN timing has not, to our knowledge, been evaluated, but is expected to be small (WAIT, 1969, 1971).

Speed of Light in Free-Space

The speed of light (C_0) in free-space adopted by the International Union of Geodesy and Geophysics, IUGG (1975), and by the USCG (1980) for LORAN is given in Table 1. Note that this is not the same value used by JOHLER et al. (1956) which is 8.81 ppm faster. The change in C_0 is equivalent to a change in the nominal index of refraction discussed next.

TABLE 1

Effective propagation speeds for light in a vacuum (top), for DECCA and LORAN in the atmosphere (center), and for the RTCM (1981) LORAN SALT-model approximation of various ranges (bottom)

PPM	Source	Value km/sec.	Comments
- 9	JOHLER et al. (1956)	299,795.1	C_0 (1956)
0	USCG (1980)	299,792.458	C_0 (1975)
65	ASLAKSON (1964)	299,773	C_0 (1940 s)
309	IHR, LAURILA (1956)	299,700	Ocean, DECCA
322	LAURILA (1956)	299,696 \pm 26	Ocean, DECCA
338	USCG (1980)	299,691.16	C_0 (1975) + 1.000338
475	LARSSON (1949)	299,650	Ocean, DECCA
505	LACROIX & CHARLES (1960)	299,641	Ocean, DECCA
609	GRAY (1977)	299,610 \pm 15	Ocean, DECCA
602	BRUNAVS & WELLS (1971 a)	299,612 \pm 28	Ocean, DECCA, 185 km
682	BRUNAVS & WELLS (1971 a)	299,588 \pm 28	Ocean, DECCA, 375 km
746	LONARS, JERARDI (1982)	299,569 \pm 12	Ocean, LORAN
809	DEAN et al. (1962)	299,550 \pm 12	Ocean, LORAN, 812 km
913	DEAN et al. (1962)	299,519 \pm 9	Ocean, LORAN, 1 840 km
1234	SALT-model	299,423	20 km range
666	SALT-model	299,593	100 km
786	SALT-model	299,557	500 km
870	SALT-model	299,532	1 000 km
926	SALT-model	299,515	2 000 km

Index of Refraction, n , and Refractivity, N

The index of refraction (n) of radio waves in a medium is the ratio of the phase speed in free-space, C_0 , to that in the medium C

$$n = \frac{C_0}{C} \quad (8)$$

Because n in air typically has values ranging from 1.000250 to 1.000450, it is convenient to define the refractivity (N) as

$$N = (n - 1) \times 10^6$$

Thus N for air is in the range 250-450.

Some representative values of N (BEAN and DUTTON, 1966) are :

	\bar{N} Feb.	\bar{N} Aug.	σ_N Feb.	σ_N Aug.
Denver.....	245	277	4	15
Boston.....	309	350	5	15
Miami	330	380	14	6

Here \bar{N} is the monthly mean value of 8 years and σ_N is the standard deviation of the monthly means. On the U.S. East Coast, the extremes of the monthly mean values of N are about 50 N -units. Extensive tables and charts of many aspects of N -meteorology are also given by BEAN and DUTTON (1966).

Figure 3 illustrates the data given in Table 1. Three values for the speed of light in vacuum from the 1940s, 1956, and 1975 are shown at the top. Various estimates of the effective speed \bar{C} of radio propagation (ratio of arc distance travelled to total travel time) are shown as a function of range from the transmitter. The DECCA values are shown as published (or inferred from the published data) without correction from DECCA frequencies to the 100-kHz nominal value of the LORAN and SALT-model data. The correction is both range and frequency dependent, but typically will reduce the DECCA \bar{C} 's by about 18 km/sec. The curve marked "SALT-model" shows the predicted effective speed at 100 kHz using the technique of BRUNAVS and WELLS (1971 b). Example PF, SF, and ASF corrections are shown to suggest the relative size of each. The ASF corrections shown (inset) are for all land paths and are generally larger than the mixed land-sea paths of nearshore transmitters. Speed changes due to monthly mean n variations for three cities are given above the inset.

Historically, there has been a selection bias in reporting new observations of the speed of light (ASLAKSON, 1964; SANDERS, 1965; and FROOME and ESSEN, 1969). If one is close to the accepted value, he stops work and publishes; if he is not close, he tends not to publish. Thus, published values of C_0 for various decades have tended to cluster. A similar selection process may also be present in some of the radio ground-wave propagation velocity literature.

Values of n in air vary with pressure, temperature, and humidity. Thus, location, altitude, barometric pressure, time of day, weather, climate, etc. alter n . The relation of N to the absolute temperature (T) in degrees Kelvin, the total pressure (P) in millibars, and the water vapor pressure (e) in millibars is given by SMITH and WEINTRAUB (1953), BEAN and THAYER (1959), BEAN and DUTTON (1966), and the CCIR (1978) as :

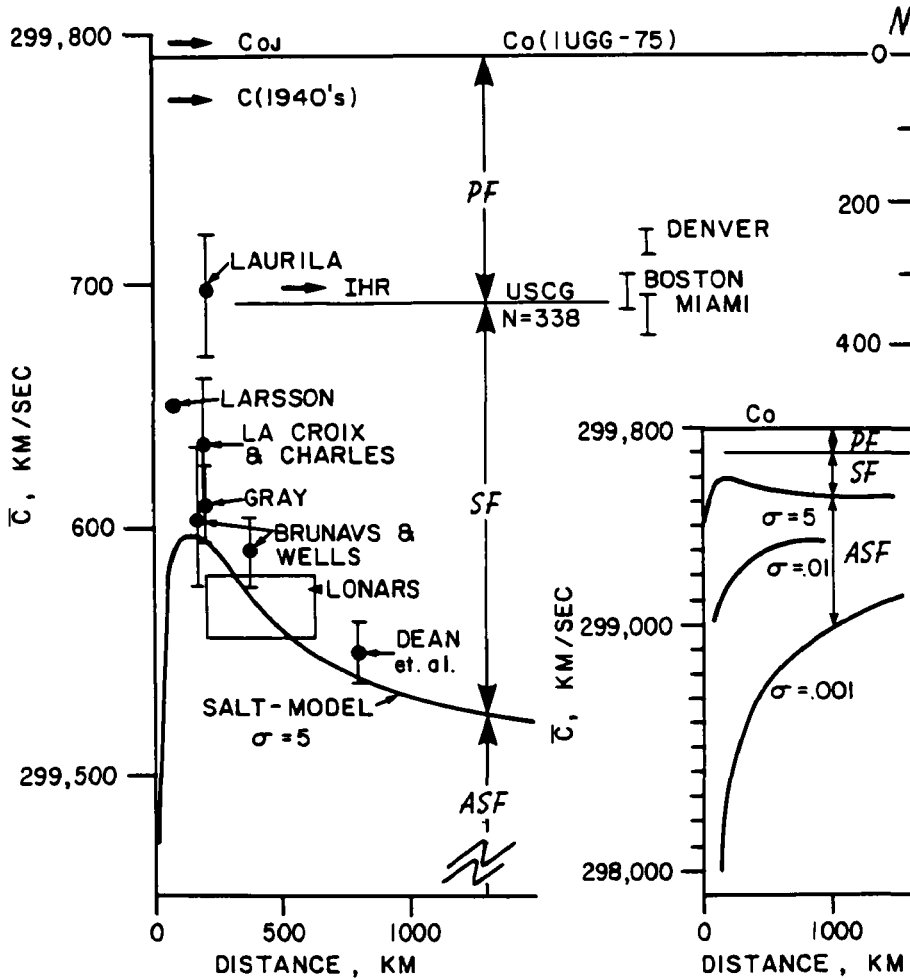


FIG. 3. — Effective propagation speeds \bar{C} listed in Table 1 versus distance are indicated (left). Monthly mean variations of \bar{C} due to index of refraction variations are shown for Denver, Boston and Miami. The inset figure (lower right) shows the PF, SF, and ASF corrections at reduced scale.

$$N = \frac{77.6}{T} \left(P + \frac{4810e}{T} \right) \tag{9}$$

Because e increases very rapidly with T in the range of interest ($\sim T^{18}$), N increases with temperature in humid air. Equation 9, derived from theory and laboratory measurements, is thought to accurately model N to within one N -unit. Instrumental errors in the determination of P , T , and e , however, limit practical accuracy to about ± 4 N -units. Direct measurements with radio-frequency resonators allow about an order of magnitude improvement in resolution.

Figure 4 shows the speed of propagation (C) for representative values of P , T , and humidity calculated from equation 9 and standard tables of water vapor pressure. Notice the large (100 ppm) change in C from 0 to 100 percent humidity at room temperature.

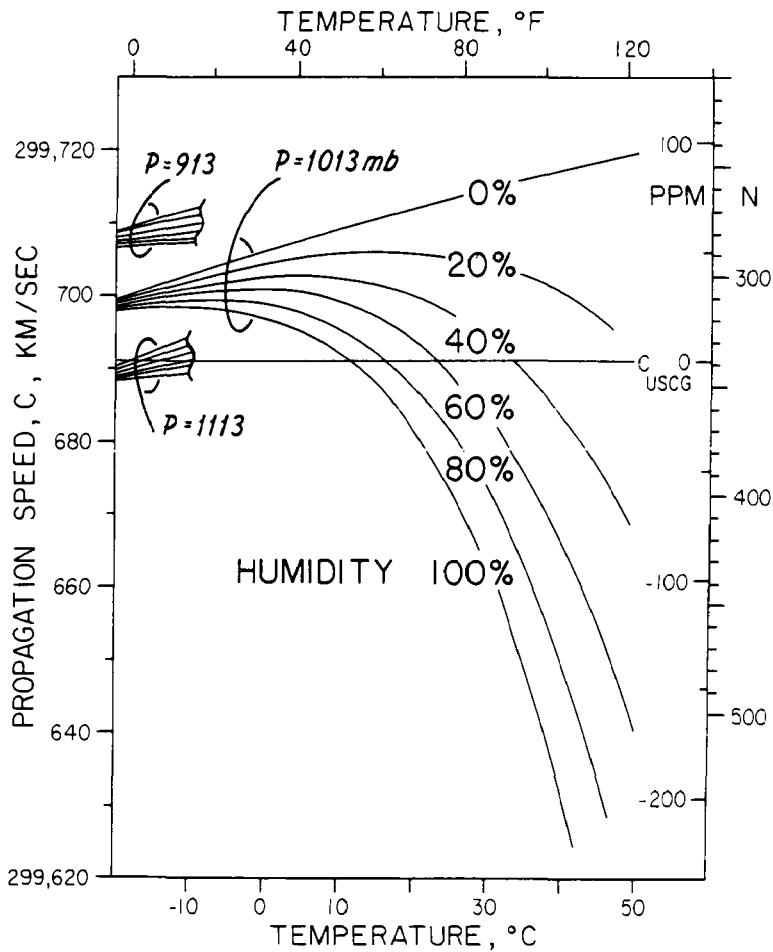


FIG. 4. — Variation of radio propagation speed with atmospheric pressure, temperature, and humidity. Scales of refractivity (N) and changes in parts per million (ppm) are shown at right. Pressure changes are suggested by truncated families of humidity curves at left.

As noted above, the arbitrary nominal value of n as adapted by the USCG is 1.000338. (This value is from JOHLER et al., 1956, p. 37, wherein $n = \sqrt{\epsilon_1}$, and apparently in turn from SCHULKIN, 1952, for summer conditions near Washington, D.C.). As seen in the figure, this is a reasonable nominal value in the range of general interest at sea. We wish to emphasize that this USCG value for n is a nominal model definition, not a measurement, and, as such, it serves the function of uniform normalization for the LORAN community. It may not represent the best nominal value, particularly in the tropics, at higher altitudes, or for aircraft. Perhaps more representative seasonal and regional values could be established as well. Alternately, n can be estimated directly from weather observations and charts.

Effects of n Aloft

The net LORAN propagation rate at the earth's surface is influenced by

propagation modes moving at higher altitudes and hence is influenced by values of n aloft. The index of refraction decreases from its surface value, slightly greater than unity, to exactly unity in free-space. The decrease of n with altitude refracts the signal toward the earth. Refraction and diffraction around the earth then allow over-the-horizon ground-wave transmission.

From 888 sets of monthly mean balloon soundings from 45 U.S. weather stations, BEAN and THAYER (1959) show an exponential decay of N with altitude such that :

$$\Delta N = - 7.32e^{0.05577N_s} \quad (10)$$

where ΔN is the difference between the surface refractivity (N_s) and that at 1 km above the surface. The strong coupling of N_s and ΔN allows one to estimate the N -field near the earth without direct measurement aloft for most of the contiguous United States with the exception of southern California during the summer months.

The Van der POL-BREMMER method, however, assumes a *linear* change of N with altitude. This convenient fiction gives surprisingly good results (BEAN and THAYER, 1959) because most of the refraction of the low-angle ground-wave rays occurs in the lower atmosphere. The method then finds the radius of an "equivalent" earth (a_e) such that curvature of the real earth ($1/a$) plus that due to Snell's law of refraction in the linear gradient of n with height (h) dn/dh , is

$$\frac{1}{a} + \frac{1}{n} \frac{dn}{dh} \cos \theta = \frac{1}{a_e} \quad (11)$$

where θ is the elevation angle of the ray, a is the earth radius, and n is the surface index of refraction. The method then introduces the factor alpha such that

$$\alpha = \frac{a}{a_e} = 1 + \frac{a}{n} \frac{dn}{dh} \quad (12)$$

Finally, the value a_e is arbitrarily taken to be $4/3 a$ ($\alpha = 0.75$) without further regard for N_s or the profile of N . It is not clear that the $4/3$ model is the best nominal value at 100 kHz (CCIR, 1978). Table 2 shows α calculated from equations 10 and 12. Note that the arbitrary selections of $\alpha = 0.75$ and $n = 1.000338$ are

TABLE 2

Mean surface refractivity N_s ,
vertical gradient of refractivity ΔN and the Bremmer factor α

N_s	ΔN	α	$\alpha^{2/3}$
200	- 22	0.86	0.90
250	- 30	0.81	0.87
300	- 39	0.75	0.83
350	- 52	0.67	0.77
400	- 68	0.57	0.68
450	- 90	0.43	0.57
338	- 48	0.69	0.78
301	- 39	$(4/3)^{-1}$	0.83

inconsistent ($\alpha = 0.75$ corresponds to $N = 301$, not 338) with the model of equation 10.

Such historical oddities suggest it may be time to review the nominal values used in the DMA/USCG method as well as the method itself. Are the nominal values consistent and representative? Might regional and seasonal coefficients improve performance? What are the general parametric sensitivities of the various terms of the method? How do its predictions compare with those of other models and observations? Partial answers to such questions exist in the literature; a definitive study is not yet available.

Conductivity

The propagation rate is affected by the complex impedance of the air-earth boundary layer with a skin depth ranging from about 0.75 m for sea water to more than 50 m for dry land. The land electro-magnetic boundary effects are determined by the curvature of the earth, the roughness of the terrain at the scale of the transmitted wave length (3 km) and the equivalent impedance of the ground. The impedance depends on the rock type, penetration depth, stratification, soil type, and, in particular, on the rock and soil moisture content. Such electrical effects are used for geo-electromagnetic prospecting (ROKITYANSKY, 1982, and WAIT, 1982). Typically, the travel-time variations are caused by changes in the resistive or conductive component of the impedance.

The integrated impedance effects over a zone are conventionally modeled as a single bulk conductivity determined empirically for that zone. The integrated effects over various zones are then estimated by MILLINGTON's (1949) method discussed below. Effects of mountains, woods, and buildings are lumped together with the impedance effects by ad hoc adjustment of the effective conductivities.

Values of conductivity (mhos/meter) range from about 0.001 for dry earth to 0.010 for marshy woodland and sea ice. Water conductivity ranges from about 0.001 to 5 or more in the ocean (TERMAN, 1943). Mountains, woods, and buildings tend to reduce the effective conductivity (GUPTA and ANDERSON, 1979; and JOHLER et al., 1979). GRANT (1977) shows that the effective conductivity may change by a factor of 2 from a dry to a wet year, but short-period effects of heavy rains are relatively small, as LORAN waves penetrate well below the storm-wetted layer. At a range of 10^6 m, the travel-time is about 3,338 microseconds over the ocean. If the path were over smooth land, the travel-time would be increased by only about 5 microseconds, but LORAN surveyors require travel-times accurate to 0.1 microsecond or better, i.e., to about 30 ppm. This requires that we know the effective land delays to a few percent.

Land Delay Models

A number of interesting propagation models for LORAN and other electromagnetic waves have been developed since the first efforts early in this century (SAMADDAR, 1980; WAIT, 1964; and WAIT, 1981). The MILLINGTON (1949) semi-

empirical model (and its extension to phase by PRESSEY et al., 1956) is used by DMA. It combines relative computational simplicity with accuracy limited mainly by the empirical input constants, i.e. the effective conductivities of the ground segments. The delays for each segment are estimated in both directions, assuming a smooth homogeneous earth of conductivity equal to that of the segment. The model then sums and averages the nonlinear range-dependent delays to the receiver and, in the opposite direction, back to the transmitter. The rationale for this procedure (Fermat's principle) is nicely described in some detail by MONTEATH (1973).

The Millington model requires about half a page of BASIC-code and runs on an Apple II calculator in 10-20 seconds of computer time per estimate. Conductivity models utilizing only two segments give offshore results similar to those of the more detailed geometry used by DMA in large computers. For ships, the radial ASF predictions need only be updated every half hour or so, making both the computational and programming requirements small. The difficulty, therefore, is neither the model complexity nor the computing time, but the selection of appropriate conductivity boundaries and values.

Model Predictions

Model ASF's for the New York Bight area (DMA, 1981) are contoured in Figure 5. The DMA X-TD model data shown use detailed geography with five fixed conductivities (0.0005, 0.003, 0.005, 0.03 and 5.0 mhos/m). Because the transmissions from Nantucket Island are nearly all over water, the contoured corrections are very nearly those of the ASF's due to Seneca alone. The published data end at the Coastal Confluence Zone (CCZ) but are easily extended indefinitely to sea by the model.

COMPARISON OF THE MODEL WITH OBSERVATIONS

Nearshore

Observed nearshore effects are interestingly described by PRESSEY et al. (1956) for DECCA transmission (CW) in England. They find 5°-10° (about 0.2 microseconds) complex spatial phase variations within six wavelengths (18 km) of shore; most of the effect is in the first three wavelengths. These spatial undulations occur, as might be expected, where the abrupt changes in boundary conditions excite higher order propagation modes which then decay rapidly with distance.

Figure 6 repeats the model delays shown in the dash-dot box of Figure 1, together with observations taken at sea and ashore. Four types of observations were used: a) Land survey data taken at two locations in an open field at the USCG station at Watch Hill, R.I., using an Internav 404 receiver and local survey control converted to WGS-72; b) USCG survey observations using Austron 5000 receivers and Maxiran navigation from shore stations (MILLER et al., 1981, and WESEMAN,

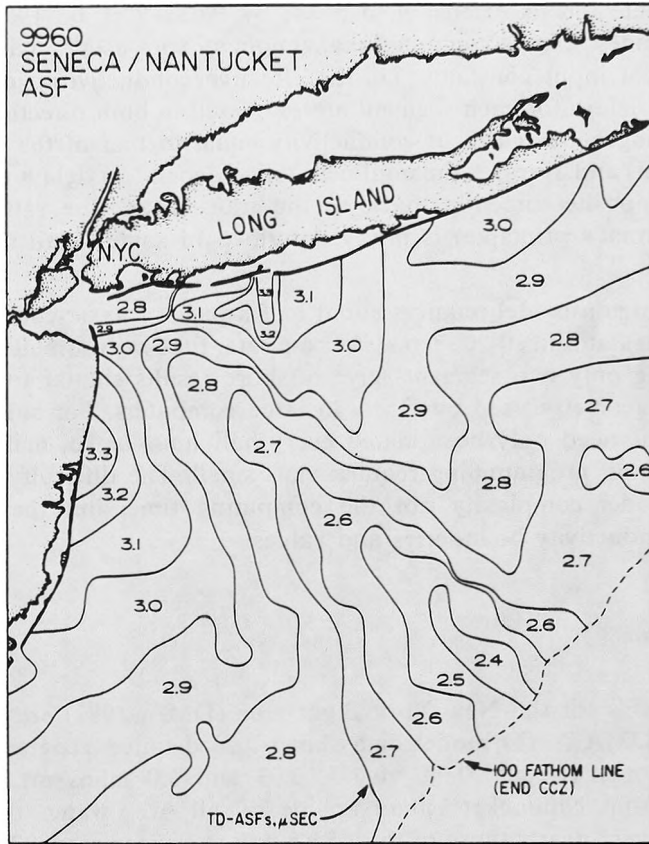


FIG. 5. — Contours of modeled overland delays (ASF's) in the New York Bite area. TD variations for Nantucket primarily reflect land effects from the master transmitter at Seneca, NY. Data is from DMA (1981).

1982 a, 1982 b); c) A single mean estimate derived from time series of Internav 404 LORAN fixes and baseline crossing data; d) The average of 26 simultaneous Northstar-6000 LORAN and JMR-4a Transit satellite fixes. The observational data shown are in general agreement with the model ASF at about the 0.1-microsecond level; however, the model curve does not include ASF delays from the Nantucket transmitter which are included in the observed X-TD on rate 9960 shown.

The complexity of the nearshore effects probably limits model predictions to the ± 0.1 -microsecond level nearshore or perhaps twice this near rugged shores (EATON et al., 1979). In addition, the Millington model introduces offsets of about 0.1 microseconds nearshore (BRUNAVS, 1976). Amplitude and phase measurements made in the vertical from aircraft would aid the model calibration and allow prediction beyond restrictive political boundaries.

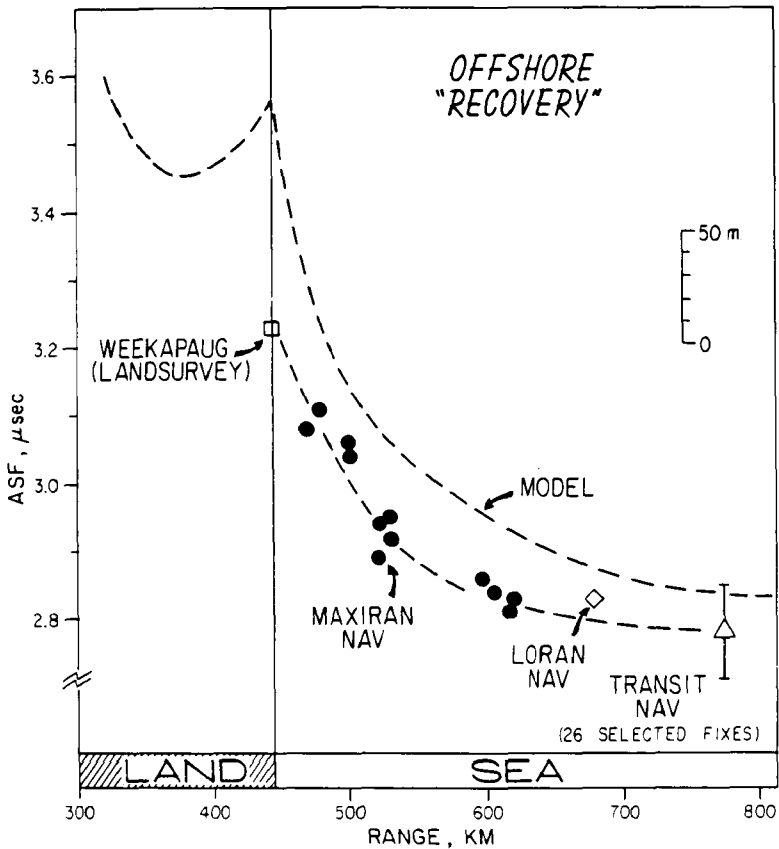


FIG. 6. — Model and offshore phase recovery observations are compared for the Seneca-9960, 108° azimuth radial shown in the dash-dot area of figure 1, near Weekapaug, RI. Four different types of X-TD observations show a systematic trend similar to, but slightly displaced (0.1 microseconds) from the model prediction.

Far Offshore

How accurate are the ASF model predictions? We have given considerable attention to this question for the 9960-Chain and summarize our results in Figure 7. Several thousand simultaneous Transit satellite and LORAN fixes have been collected, edited and reduced to the nine sets of 219 observations shown in the figure. All observations were made from June to October when n and SAM anomalies are usually smallest. Figure 8 shows the X-TD residuals versus the azimuth at Seneca. The Y-TD residuals listed show a similar distribution except for area 7.

Test areas 3, 4, 5 and 9, surveyed with different ships and receivers in three separate years in a $\pm 5^\circ$ band near Seneca azimuth 140 degrees (figure 8), are consistent for both X and Y TD's at the 0.1-microsecond level. Paths from the X and Y transmitters to areas 6, 7, 8 and 9 are nearly all over water, so the unknown

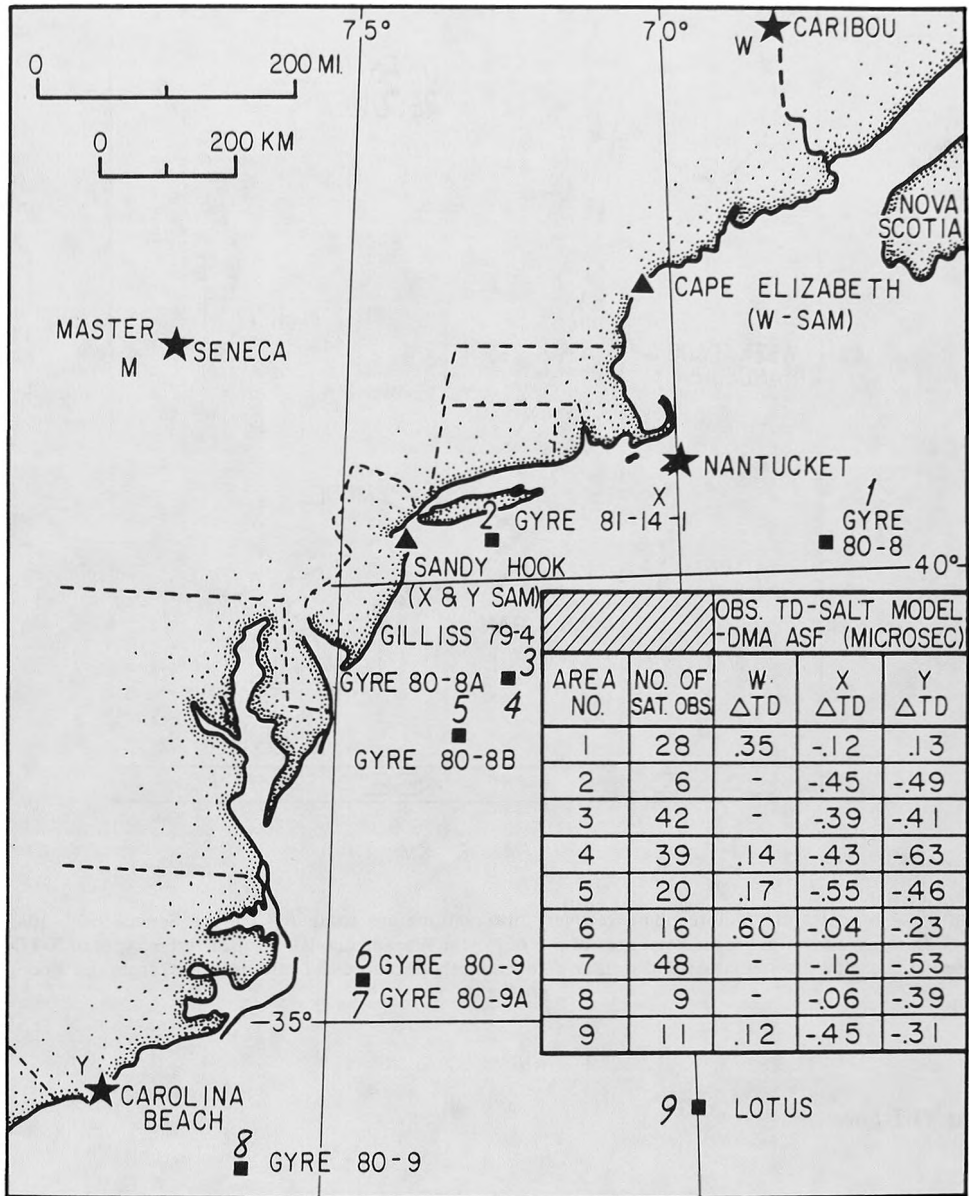


FIG. 7. — Residuals of observed values less model predictions for 9 offshore areas of Loran Rate-9960. The residuals are based on Transit satellite observations and ASF predictions using DMA model conductivities.

effects of the path delays from M can be eliminated by differencing the X and Y TD's. The resulting systematic trend merits further investigation. The signs of the W corrections are opposite to those for X and Y, suggesting that the primary ASF residuals from the DMA model for 9960 are on the Seneca and Caribou radials. It would be useful to have time series and spectra for periods of a year and longer of TD's and TOA's taken at fixed monitors at sea — possibly on oil platforms,

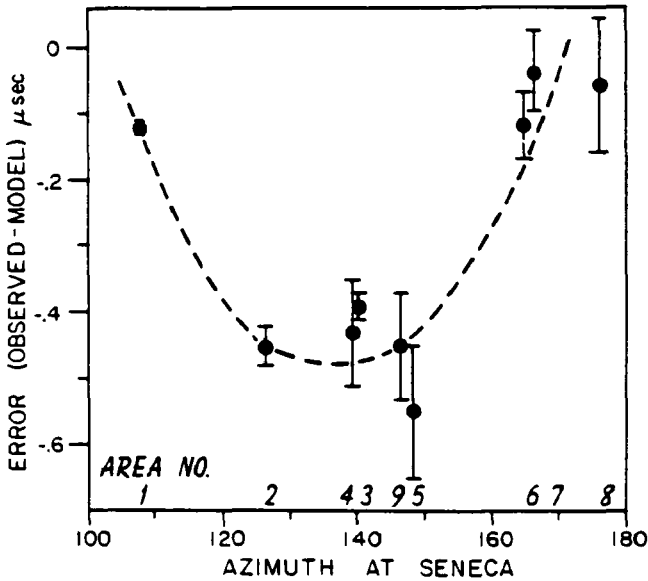


FIG. 8. — Trend of X- Δ TD residuals of the previous figure. Scatter over 3-year period near azimuth 140° is of the order of 0.1 μ sec. Tentative systematic trend is suggested by arbitrary dash line sketched. Error bars represent \pm one standard error of the means. Area numbers are shown along X-axis.

buoys, lightships, and on offshore islands. Additional details of the azimuthal structure nearshore are provided by the recent USCG ship surveys (see USCG Radionavigation Bulletin, numbers 10 and 11).

SF AND ASF CONSIDERATIONS

Saltwater Correction, SF

The algorithm recommended by the RTCM (1981) and in general use by DMA is a two-segment polynomial fit (HARRIS, 1964) to Tables 18 and 20 of JOHLER et al. (1956).

Table 3 shows the residuals of the fit to the tabulated values in JOHLER et al. (1956) and to direct computations by BRUNAVS (1976, 1977). As seen in the table, there is a large discontinuity at 100 statute miles between the near field (flat earth) and far field (spherical earth) models. No significant discontinuity, however, is seen with BRUNAVS' values. Further comparison with BRUNAVS' values shows a cyclic residual of the fit with peaks of -21 , $+17$, and -3 nanoseconds at 155, 497, and 1,864 statute miles, respectively. *Below 1 mile or so, the RTCM model should not be used.* The residuals are unfortunately largest (± 6 m) in the 50-500 mile range, our primary interest at sea. The BRUNAVS and JOHLER model coefficients are not always those in present use by the USCG.

TABLE 3

Residuals to the DMA-RTCM proposed fit. Columns 1 and 2 list the distance and SF correction from JOHLER et al. (1956, Tables 18 and 20). Columns 3 and 4 indicate the difference between the RTCM (1981) fit and the JOHLER et al. (1956) tables (RTCM-JOHLER). Column 5 gives the difference or bias between the RTCM (1981) fit and the direct BRUNAVS (1977) solution (RTCM-direct)

DISTANCE	SF	FIT RESIDUALS		BIAS
s. miles	$\mu\text{sec.}$	$\mu\text{sec.}$	m	m
0.1	4.4209	+ 0.672	+ 201	—
0.2	3.5802	— 1.039	— 311	—
0.5	1.1807	— 0.170	— 51	—

1.0	0.5038	— 0.003	— 1	—
2.0	0.2448	+ 0.003	+ 1	+ 1
5.0	0.1032	— 0.004	— 1	— 2
10.0	0.0593	— 0.002	— 1	— 3
20.0	0.0409	+ 0.008	+ 2	— 2
50.0	0.0368	+ 0.050	+ 15	— 1
100.0	0.0434	+ 0.126	+ 38	— 4

100.0	0.1755	+ 0.004	+ 1	— 1
200.0	0.4205	— 0.015	— 4	— 6
500.0	1.3579	+ 0.017	+ 5	+ 6
1000.0	3.0811	+ 0.004	+ 1	+ 2
2000.0	6.5466	— 0.005	— 1	— 1

In short, the conversion from distance to time is considerably less accurate than is the distance determination alone. This will have practical implications for computer accuracy, speed, etc., for LORAN receiver manufacturer's development of latitude/longitude converters. The geodetic distance, of course, is not the distance traveled by the radio waves, but acts only as a scaling parameter in the effective speed calculation. The corrections to the actual distances traveled are absorbed in \bar{C} .

ASF Definitions

The phrase, Additional Secondary-phase Factor (ASF), has grown to mean land-induced propagation delays. Laying aside, for the moment, the interpretative problems associated with the phase of a zero-crossing time measurement of a broad-band pulse, let us consider ASF as a generic term referring to land-induced propagation travel-time delays — a sort of spatial-temporal-modal mean-time interval. In this context, we look next at four of the several ASF definitions now in use.

Range ASF. The USCG (1980) definition of ASF is :

“The amount, in microseconds, by which the time difference of an actual LORAN signal that has traveled over varied terrain differs from that of an ideal signal which has been predicted on the basis of travel over an all-seawater path. (LORAN signals travel slower over ground.)”

This is the clearest use of the term, i.e., the additional travel-time from one transmitter antenna to one receiver antenna relative to that calculated from a standard all-salt-water model of the path. It is the anomaly of the travel-time component relative to an arbitrarily defined propagation SALT model.

$$ASF_R = PATH_{TT} - SALT_{TT}$$

The range ASF is equal to the actual (or best estimate) travel-time over the path less that predicted by the standard SALT-model. The net delays are caused mostly by land effects; but lakes, bays, and even ocean segments contribute to the sum of the nonlinear segment delays of the total travel-time and, hence, to the range ASF.

One need not be concerned with how representative the SALT-model is relative to local conditions (season, weather, topography, etc.); the model is only used to form a reference travel-time that accounts for most of the air and planetary boundary effects in a computationally expedient fashion. Note that although some salt-water propagation model is implied, a LORAN-chain model is not. Conceptually, one could directly determine such an ASF by measuring the mean actual travel-time with a portable clock. Comments on the nature of any particular mean (ground cover, ice, N_s , N-profile, number of observations, averaging methods, equipment, etc.) would complete the ASF estimate. Such measurements are now periodically made in the LORAN-C Emission Delay calibration. The results, however, are not generally presented as the ASF's of the baselines.

Delta ASF. The delta ASF is simply the difference between two range ASF's :

$$\Delta ASF = ASF_{R2} - ASF_{R1}$$

The published DMA (1981) Loran-C Correction Table is computed in this way relative to the DMA SALT-model first published by the RTCM (1981).

The Observed or TD-ASF. The observed or TD-ASF is the difference between the observed TD and the SALT-model TD at a location. It includes all causes of TD variations in the LORAN-chain. Operationally, it is much easier to measure than the range-ASF, but should not be confused with it. The TD-ASF might better be called a TD correction and is :

$$ASF_{TD} = OBS_{TD} - SALT_{TD}$$

Note that this definition implies a Master/Secondary LORAN model as well as the SALT-model. (It is necessary to know the emission delay and SAM steering effects due to weather, ice, seasons, etc., in order to relate the observed TD to a nominal TD for the location.)

The RTCM (1981, p. 1) defines ASF as :

“The amount, in microseconds, by which the time difference of an actual pair of LORAN-C signals that travel over terrain of various conductivities differs from that of signals which have been predicted on the basis of travel over all-sea-water paths.”

Although the wording is nearly identical with that of the USCG Range ASF definition above, the meaning has been changed to that of the TD-ASF.

The SAM-ASF. The TD-ASF at the SAM is an indirectly defined value set by the coordinates of the SAM antenna and the defined CSTD value. The TD-ASF at the SAM is held constant by changing the Emission Delay of the Secondary. The form of nominal ASF corrections such as those of Figs. 5, 7, and 8 are influenced by the arbitrary selection of the SAM-ASF.

It seems unnecessary to attempt to alter the varied general usage, but for mathematical clarity, some rigorous definitions are needed.

ASF Sign Conventions

Both positive and negative sign conventions are used for ASF's. DMA shows all additional secondary phase factors (ASF's) as negative whereas secondary phase factors (SF's) are considered positive; yet, both increase the travel-time. When considered as receiver corrections, however, the ASF's used to adjust the observed TD's to positions charted from SALT-model predictions are negative. It is important here to distinguish between model anomalies and TD corrections.

Published ASF's (DMA)

DMA has calculated ASF's for military applications for many years. In April 1981, these values and the conductivities used to calculate them were declassified. DMA now offers LORAN-C correction tables for rates 5930, 9960, 8970, 7980, 9940, 5990, 7960 and 9990 (USCG, Radionavigation Bulletin). The published ASF values are for the CCZ from nearshore to the 100-fathom line, on a 5-arc-minute latitude/longitude (~ 5 mile) grid. With the exception of 9940 in Southern California, the ASF's are Millington model calculations based on USCG conductivity maps and do not include observations taken during the USCG LORAN verification surveys. Revised tables that include a "force-fit" of the offshore calibration data, but do not necessarily represent an adjustment of the model conductivities, are being prepared by DMA.

The next step might be to use tomographic or inverse techniques to adjust the model input parameters for a best fit to the weighted observational data available in each chain. GRESSANG and HOROWITZ (1978) proposed using a Kalman filter approach for such an adjustment. Although conceptually feasible, the conductivity adjustment procedures have not been implemented in the DMA LORAN ASF modeling.

OTHER CONSIDERATIONS

Temporal variations, SAM control procedures, and unmodeled terms all contribute to the observed errors. At Woods Hole, Mass., we routinely observe Time-of-Arrival (TOA) standard deviations of 7-40 nanoseconds for 2-hour averages at ranges of 40-780 nautical miles over water on rates 9960 and 5930. In

addition to the ASF correction, it is probably appropriate to make at least SAM, seasonal, and catch-all corrections for survey applications. In the last 20 years, the accuracy of the Transit satellite system on land has improved from about 2 000 m to better than 1 m, largely through improved error models.

Weather and Seasonal Effects

Variations of several tenths of a microsecond of TOA measurements can accompany weather fronts. The variations observed at Woods Hole typically reach a maximum in about an hour and take several hours to recover. The controversial issue of storm and seasonal variation is discussed in CAMPBELL et al. (1979), CHARRON (1981), CREAMER and DePALMA (1981), DOHERTY et al. (1979), EATON et al. (1978), ILLGEN et al. (1979), ILLGEN and FELDMAN (1978), MUNGALL et al. (1981), POLHEMUS (1981), POTTS and WIEDER (1972), SAMADDAR (1980), WARREN et al. (1978), WINKLER (1972), and the referenced literature extending back into the 1950's. The longstanding puzzle concerning the size and cause of such effects now seems to favor about a one-microsecond peak-to-peak seasonal variation per 500 km in New England with the primary cause being seasonal variations of n and α in addition to ground conductivity changes.

Effects Longer Than One Year

GRANT (1977) observed variations in the ASF correction from 1972 to 1975 of 0.004-0.002 mho/m and noted they "may be due to the different meteorological conditions between the two years (1972 was notably wet while 1975 was notably dry)." The offset shown results in a range error of order 100 to 200 m for DECCA navigation over Newfoundland. The USCG (1982) monitors should allow detailed modeling of such effects, which were seen clearly in various other studies such as DOHERTY and JOHLER (1975).

System Area Monitor (SAM) Considerations

SAM control effects can be illustrated (Fig. 9) by a simplified model in which the TDs at the SAM and observer position are :

$$\begin{aligned} \text{TD}_s &= T_2 - T_1 + (\text{ED} + t) \\ \text{TD}_p &= T_4 - T_3 + (\text{ED} + t) \end{aligned}$$

and the difference of these TDs is :

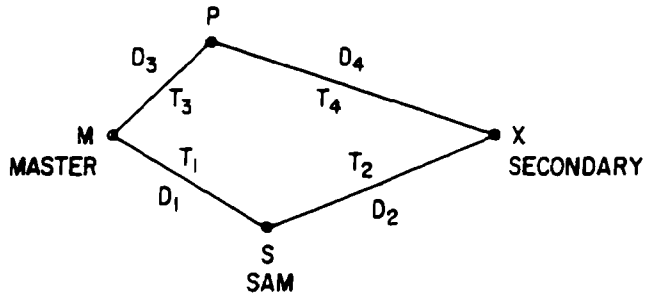
$$\text{TD}_p - \text{TD}_s = (T_4 - T_3) - (T_2 - T_1)$$

or

$$\Delta \text{TD} = \text{TD}_p - \text{TD}_s = \left[\left(\frac{D_4}{C_4} - \frac{D_3}{C_3} \right) - \left(\frac{D_2}{C_2} - \frac{D_1}{C_1} \right) \right] \quad (13)$$

If all the \bar{C} 's in equation (13) change proportionally by a constant K then :

$$\Delta \text{TD} = \frac{1}{K} \left[\left(\frac{D_4}{C_4} - \frac{D_3}{C_3} \right) - \left(\frac{D_2}{C_2} - \frac{D_1}{C_1} \right) \right] \quad (14)$$



M = Master Station
 X = Secondary Station
 S = SAM
 P = observer's location

D₁..... D₄ = length as shown

T₁..... T₄ = LORAN travel times

C₁..... C₄ = mean propagation speeds along each of the paths

TD_S and TD_P = time differences as S and P, respectively

ED = nominal emission delay at X

t = time correction at X needed to keep the TD at the SAM constant

FIG. 9. — Simplified model of SAM control.

and the ΔTD change at P is seen to be proportional to $1/K$, and the farther we are from the control TD (quantity in large brackets) the greater the change with K.

In actual use, the paths, $D_1 \dots D_4$ usually lie over different combinations of land and water which show significant seasonal and storm variations in $\overline{C_1} \dots \overline{C_4}$, causing lines of constant TD to move horizontally in a complex manner suggested by equation (13). For modeling purposes, one might separate these effects into regional and local components. For practical applications such as harbor navigation, local reporting of the TD grid corrections may become as commonplace as tower barometric corrections are for aircraft altimeters. To be widely used, the correction vectors should be simple to receive and apply. From an operational point of view, they would be best implemented as TD offsets.

Because TDs can be controlled at only one point, it seems reasonable to locate this point near the area of greatest user activity in the chain. Then, at least that vicinity needs little or no LAM or differential LORAN-type correction. If, on the other hand, the Emission Delay were held constant, only areas along the baseline extensions and near the baseline ASF mid-point would show small variations. The baseline extensions are of no use for other reasons and the baseline ASF mid-point is relatively stable anyway (equation 13). Thus, while conceptually less satisfying, an observational rationale can be made for constant CSTDs and variable EDs.

Pulse versus CW

LORAN propagation models are based on continuous wave (CW) phase assumptions, although the actual information comes from zero crossing time

differences of a 20-kHz-wide pulse. As the ground wave is weakly dispersive, i.e., the propagation speeds depend somewhat on frequency, it is interesting to evaluate the correction anticipated between the CW model and the real LORAN pulse. For ranges of 1, 100, and 500 km, JOHLER et al. (1979, Part II, p. 25) estimate corrections of + 0.11, + 0.09, and + 0.03 microseconds, respectively, over smooth homogeneous ground. Errors at ranges less than a few kilometers from the transmitter are large for other reasons, but the errors shown at 100 and 500 km are significant and should be included in a detailed error budget. The logical distinction between signal, group, and phase velocity is described in many texts (i.e., STRATTON, 1941; and WINKLER, 1972). FEHLNER et al. (1976), and JESPERSEN (1979) discuss possible methods of circumventing LORAN dispersion problems.

Height Gain

The height of the antennas above the ground and the elevation of the ground above sea level affect the propagation rate. Such effects are treated in the Van der POL-BREMMER method, but are neglected in the DMA (1981) predictions. It would be useful to formally evaluate these effects for various situations.

Geodetic Datum

LORAN-C coordinates are given in World Geodetic System 1972 (WGS-72), whereas U.S. charts and maps use the North American Datum 1927 (NAD-27). Conversion from one system to the other is provided by the Molodenski formulas summarized in STANSELL (1978) and shown graphically for the United States in STANSELL (1973). Along the East Coast, residual errors after conversion by this method are estimated to be 10-20 m; they were found to be 11 m at Woods Hole, Mass. when the global ΔX , ΔY , ΔZ offsets of STANSELL (1978) and MEADE (1982) corrections were used. Conversion by DMA charts reduces this error to a few meters (about 3 m at Woods Hole). Several general texts (HOAR, 1982; and TORGE (1980) and particularly the three International Geodetic Symposia on Satellite and Doppler Positioning at Las Cruces NM-1976, Austin TX-1979 and Las Cruces NM-1982 provide background information.

Before 1976, LORAN WGS-72 station coordinates were derived from on-site DMA Precise Ephemeris (PE) Transit Satellite Geodesy. More recently, Broadcast Ephemeris (BE) have been converted to WGS-72. Transit satellite navigation at sea utilizes the (BE), which require a small correction to convert to WGS-72 (JENKINS and LEROY, 1979; and MEADE, 1982). Nearshore, we use NAD-27. In Canada and the United States, the change in 1984 to a new standard coordinate system should help eliminate confusion in the long run, but will add another system in the interim.

GDOP, ECD, Interference and Receivers

LORAN lines of position (LOP's) generally do not cross at right angles and are thus correlated. The fix becomes less accurate with small LOP crossing angles and

with the hyperbolic spreading of the lines with distance from the transmitters. The TD's of a fix are also correlated through the shared signal from the Master and long-period noise/interference fluctuations (AMOS and FELDMAN, 1977). Changes of pulse shape (envelop to cycle difference, or ECD) are caused by frequency-dependent propagation properties and contribute significantly to the error budget. Interference, man-made and natural, is at times the dominant error source. Bridges, powerlines, buildings, etc., can significantly distort the local LORAN grid. Receiver performance is equally important. These and other topics are beyond the scope of this paper but should not be overlooked in a general error-budget analysis.

CONCLUSION AND PROSPECTUS

Our studies at sea (Figs. 7 and 8) indicate that actual LORAN performance exceeds current error-model accuracy. By renewing interest in error modeling for LORAN, we might anticipate significant improvement in accuracy. Some major points discussed are :

1. Three major advances in LORAN calibration technology have been made in the last year and a half : the DMA ASF conductivities have been declassified, the DMA ASF values have been published, and the RTCM MPS has been published (DMA, 1981; and RTCM, 1981).
2. As a next step it would be useful to reduce the DMA-ASF books to microprocessor tables or coefficients to facilitate general use.
3. The USCG monitor program can now provide the data base for SAM error models. We encourage such model development.
4. LORAN propagation theory, coefficients, sensitivity, code and worked examples should be unified and published.
5. Model results should be compared with observations and the models adjusted accordingly.
6. The present ASF predictions need to be updated. A means for adjusting the conductivities should be implemented. LAM and other input data such as the baseline ASF's should be merged to make best estimates of the ASF model coefficients.
7. The LORAN ASF calibration effort needs to be consolidated and focussed. One group should be responsible for the observations, procedures, and end products.
8. GPS will provide a superb tool for LORAN calibration and chain timing control. The improved accuracy of calibrated LORAN can be used to pace the civilian component of GPS and to serve as the primary navigation aid until GPS supersedes LORAN.

ACKNOWLEDGMENTS

It is a pleasure to thank J. LIGON, B. SCHORR, D. TAGGART, R. WENZEL and J. WESEMAN of the U.S. Coast Guard for their numerous contributions, data and valuable insights; also, E. DANFORD, L. FUNAKOSHI and B. SWARTWOOD of DMA for advice and the data used to compute ASF contours in Figure 1; and M. EATON and S. GRANT of the Canadian Hydrographic Service and D. WELLS of the University of New Brunswick for programs, papers, comments, and general encouragement. Of the numerous others who have contributed to this paper we wish particularly to thank K. CHAPMAN, H. DHAL, J. HANNA, D. HILL, S. MICHAELS, J. MORRIS, J. MOYER, and J. WAIT, as well as J. DODD, T. JERARDI, J.R. JOHLER, T. ALDRICH, G. TOLLIOS, and E. WINGET for their review of the manuscript.

REFERENCES

- AMOS, D., & FELDMAN, D. (1977) : A systematic method of LORAN-C accuracy contour estimation. The Wild Goose Association, Annual Technical Symposium, 6th, Proceedings, pp. 77-98.
- ASLAKSON, C.I. (1964) : The velocity of light. International Hydrographic Review, Monaco, Vol. XLI(1), pp. 69-83.
- APL (The Johns Hopkins University, Applied Physics Laboratory) (1981) : Coordinate conversion, robust real time filtering of LORAN-C signals, and calibration of LORAN-C at sea. Radionavigation Journal 1980-1981, Wild Goose Association, 10th Anniversary Edition, pp. 17-88.
- APL (The Johns Hopkins University, Applied Physics Laboratory) (1982) : On the calculation of geodetic arc for use with LORAN. Radionavigation Journal, Wild Goose Association, pp. 57-61.
- BEAN, B.R. & DUTTON, G.J. (1966) : Radio meteorology. NBS Monograph 92, Superintendent of Documents, Washington, DC, U.S. Government Printing Office, 163 p.
- BEAN, B.R. & THAYER, G.D. (1959) : Models of the atmospheric radio refractive index. Institute of Radio Engineers, Proceedings, pp. 740-755.
- BIGELOW, H.B. (1965) : Electronic surveying : accuracy of electronic positioning systems. International Hydrographic Review, Supplement, vol. 6, Monaco, pp. 77-112, Sept. 1965; also Proceedings, American Society of Civil Engineers, pp. 37-76, Oct. 1963.
- BREMMER, H. (1949) : Terrestrial radio waves, theory of propagation. Amsterdam, New York, Elsevier Publishing Co.
- BREMMER, H. (1958) : Propagation of electromagnetic waves. Encyclopedia of Physics (Handbuch der Physik), Vol. 16, pp. 423-639.
- BRUNAVS, P. (1976) : Investigations of effects of inhomogeneous and irregular terrain on the groundwave propagation at 100 kHz. Written communication.
- BRUNAVS, P. (1977) : Phase lags of 100 kHz radio-frequency ground wave and approximate formulas for computations. Written communication.
- BRUNAVS, P. & WELLS, D.E. (1971 a) : Accurate phase lag measurements over seawater using Decca Lambda. Atlantic Oceanographic Lab. Bedford Institute Report A.O.L. 1971-2. Unpublished manuscript.

- BRUNAVS, P. & WELLS, D.E. (1971 b) : Accurate phase lag measurements over seawater using Decca Lambda. Commonwealth Survey Officers' Conference, Paper No. F3, pp. 1-18.
- Canadian Coast Guard (1981) : A primer on LORAN-C. Marine Aids Division, TP-2659, 2nd ed., pp. 1-41. Mailing address : Place de Ville, Tower A-6, Ontario, K1A 0N7, Canada.
- CAMPBELL, L.W., DOHERTY, R.H. & JOHLER, J.R. (1979) : Loran-C system dynamic model : temporal propagation variation study. U.S. Dept. of Transportation, U.S. Coast Guard, DOT-CG-D57-79, Government Accession No. AD-A076214.
- CCIR (1978), International Radio Consultative Committee, 1978 : Propagation in non-ionized media. Recommendations and Reports of the CCIR, XIV Plenary Assembly, Kyoto, Vol. 5.
- CHARRON, L.G. (1981) : Relationships between U.S. Naval Observatory, LORAN-C and the Defense Satellite Communication System. The Annual Precise Time and Time Interval Applications and Planning Meeting, 13th, Proceedings, pp. 201-216.
- COLLINS, J. (1980) : Formulas for positioning at sea by circular, hyperbolic and astronomic methods. National Oceanic and Atmospheric Association Technical Report No. 81.
- CREAMER, P.M. & DePALMA, L.M. (1981) : Literature review of LORAN-C grid stability and warpage tests. The Wild Goose Association, Annual Technical Symposium, 10th, Proceedings, pp. 103-127.
- DEAN, W.N., FRANK, R.L. & WATTS, P.C. (1962) : Use of LORAN-C for intercontinental surveying. Intern. Hydrogr. Review, Supplement, Monaco, Vol. 3, pp. 77-84.
- Defense Mapping Agency (1981) : LORAN-C correction table. Washington, DC, Defense Mapping Agency, Hydrographic/Topographic Center, DMA Stock No. LCPUB2211200-C.
- DePALMA, L.M., CREAMER, P.M. & ANDERSON, E. (1980) : Quantification of St. Marys River LORAN-C time defence grid instability. The Wild Goose Association, Annual Technical Symposium, 9th, Proceedings, pp. 51-61.
- DOHERTY, R.H., CAMPBELL, L.W., SAMADDAR, S.N. & JOHLER, J.R. (1979) : A meteorological prediction technique for LORAN-C temporal variations. The Wild Goose Association, Annual Technical Symposium, 8th, Proceedings, pp. 152-163.
- DOHERTY, R.H. & JOHLER, J.R. (1975) : Meteorological influences on LORAN-C ground wave propagation. Journal of Atmospheric and Terrestrial Physics, Vol. 37, pp. 1117-1124.
- EATON, R.M., SCHENING, E. & STUIFBERGEN, N. (1978) : A long range performance test of LORAN-C in Atlantic Canada. The Wild Goose Association, Annual Technical Symposium, 7th, pp. 245-247.
- EATON, R.M., MORTIMER, A.R. & GRAY, D.H. (1979) : Accurate chart latticing for LORAN-C. Intern. Hydrogr. Review, Monaco, Vol. LVI (1), pp. 21-33.
- FEHLNER, L.F., JERARDI, T.W., McCARTY, T.A. & ROLL, R.G. (1976) : Experimental research on the propagation of LORAN-C signals. Vol. A : Summary Report. The Johns Hopkins University, Applied Physics Laboratory, APL/JHU TG 1298A, 77 p.
- FELL, H. (1975) : Comments on LORAN conversion algorithms. Navigation, Vol. 22 (2), pp. 184-185.
- FOCK, Y.A. (1965) : Electromagnetic diffraction and propagation problems. New York, Pergamon Press, Vol. 1, p. 203.
- FROOME, K.D. & ESSEN, L. (1969) : The velocity of light and radio-waves. Academic Press, London and New York, 157 p.
- GRANT, S.T. (1973) : Rho-Rho LORAN-C combined with satellite navigation for offshore surveys. Intern. Hydrogr. Review, Monaco, Vol. L(2), pp. 35-54.
- GRANT, S. (1977) : A user-developed integrated navigation system. International Congress of Surveyors, XV, Stockholm, Sweden, pp. 99-113.
- GRAY, D.H. (1977) : The propagation velocity of Decca-frequency transmissions over sea ice. Intern. Hydrogr. Review, Monaco, Vol. LIV(1), pp. 59-71.

- GRESSANG, R.V. & HOROWITZ, S. (1978) : Preliminary accuracy evaluation of a Loran grid prediction program. The Wild Goose Association, Annual Technical Symposium, 7th, Proceedings, pp. 87-92.
- GUPTA, R.R. & ANDERSON, E. (1979) : Application of semi-empirical TD grid calibration to the west coast LORAN-C chain. The Wild Goose Association, Annual Technical Symposium, 8th, Proceedings, pp. 82-94.
- HARRIS, L. (1964) : Polaris FBM program navigation subsystem. Brooklyn, N.Y., Lab. project 9500-1, Technical Memo 26, U.S. Naval Applied Science Laboratory (9110-P-IJ), pp. 1-11 and A1-A3.
- HEFLEY, G. (1972) : The development of LORAN-C navigation and timing. Washington, DC, U.S. Government Printing Office, National Bureau of Standards Monograph 129.
- HOAR, G.J. (1982) : Satellite surveying. Torrance, Calif., Magnavox Advanced Products Division, Brochure MX-TM-3346-81, No. 10058.
- HOWE, H.H. (1960) : Note on the solution of Riccati's differential equation. *Journal of Research of the National Bureau of Standards*, Vol. 64B, No. 2, pp. 95-98.
- HUFFORD, G.A. (1952) : An integral equation approach to the problem of wave propagation over an irregular terrain. *Quarterly Journal, Applied Math* 9, pp. 391-404.
- ILLGEN, J.D., MASON, T. & GAMBILL, B. Jr. (1979) : LORAN-C propagation and equipment timing fluctuations and conductivity estimates observed in the Great Lakes region. The Wild Goose Association, Annual Technical Symposium, 8th, Proceedings, pp. 142-151.
- ILLGEN, J.D. & FELDMAN, D.A. (1978) : LORAN-C signal analysis experiments, an Overview. The Wild Goose Association, Annual Technical Symposium, 7th, Proceedings, pp. 161-169.
- International Union of Geodesy and Geophysics (1975) : Grenoble, XVIth General Assembly, Proceedings.
- JENKINS, R.E. & LEROY, C.F. (1979) : Broadcast versus precise ephemeris — apples and oranges ? Austin, Texas, International Geodetic Symposium on Satellite Doppler Positioning, 2nd, Proceedings, pp. 39-62.
- JERARDI, T. (1982) : The LONARS-aided Doppler solution — a new method for precise positioning at sea. Proceedings of the Third International Geodetic Symposium on Satellite Doppler Positioning, pp. 755-782.
- JESPERSEN, J.L. (1979) : Some implications of reciprocity for two-way clock synchronization. Proceedings of the 11th Annual Precise Time and Time Interval (PTTI) Applications and Planning Meeting, pp. 171-184.
- JOHLER, J.R. (1962) : Propagation of low-frequency radio signals. Institute of Radio Engineers, Proceedings, Vol. 50, No. 4, pp. 404-427.
- JOHLER, J.R. (1970) : Spherical wave theory for MF, LF, VLF propagation. *Radio Science*, Vol. 5, No. 12, pp. 1429-1443.
- JOHLER, J.R., DOHERTY, R.H. & COOK, A.R. (1979) : LORAN-C pulse transient propagation. Springfield, Va., U.S. Dept. of Transportation, U.S. Coast Guard Final Report, DOT-CG-D-52-79, NTIS Ad-AO77551.
- JOHLER, J.R., KELLER, W.J. & WALTERS, L.C. (1956) : Phase of the low radio frequency ground wave. Washington, D.C., National Bureau of Standards, Circular 573.
- JOHLER, J.R., WALTERS, L.C. & LILLEY, C.M. (1959) : Low- and very low-frequency tables of ground wave parameters for the spherical earth theory. The roots of Riccati's differential equation. National Bureau of Standards Technical Note 7, PB 151266.
- LACROIX, G.W. & CHARLES, D'A.H. (1960) : The method and use of two-range Decca. *Intern. Hydrogr. Review, Supplement, Monaco*, Vol. 1, pp. 9-31.
- LAMBERT, W.D. (1942) : The distance between two widely separated points on the earth. *Journal of the Washington Academy of Science*, Vol. 32 (5), pp. 125-130.
- LARSSON, H. (1949) : Investigation of the accuracy obtained with the Decca system for survey in the Southern Baltic. *Intern. Hydrogr. Review, Monaco*, Vol. XXVI (2), pp. 25-45.

- LAURILA, S. (1956) : Decca in offshore survey. International Association of Geodesy, Bulletin Géodésique n° 39.
- MEADE, B.K. (1982) : NWL-10F versus WGS-72 Doppler results and broadcast versus precise ephemeris coordinates. Las Cruces, NM, International Geodetic Symposium on Satellite Doppler Positioning, 3rd, Proceedings, No. 11.
- MILLER, R., ILLGEN, J., WESEMAN, J. & FALCONER, R. (1981) : LORAN-C calibration of the Gulf coast and eastern seaboard. The Wild Goose Association, Annual Technical Symposium, 10th, Proceedings, pp. 17-38.
- MILLINGTON, G. (1949) : Ground wave propagation over an inhomogeneous smooth earth. Institute of Electrical Engineering, London, Proceedings, Paper No. 794, Jan. (96, Part III, p. 53).
- MONTEATH, G.D. (1973) : Applications of the electromagnetic reciprocity principle. New York, Pergamon Press.
- MUNGALL, A.G., COSTAIN, C.C. & EKHMOLM, W.A. (1981) : Influence of temperature-correlated Loran-C signal propagation delays on international time-scale comparisons. *Metrologia*, Vol. 17, pp. 91-96.
- NEWMAN, J.N. (1980) : LORAN navigation with a hand calculator. The Society of Naval Architects and Marine Engineers Symposium, Proceedings, Abstract, pp. 6-1 to 6-13.
- POLHEMUS, W.L. (1981) : LORAN-C RNAV : The best near term solution to air operations in north eastern North America. The Wild Goose Association, Annual Technical Symposium, 10th, Proceedings, pp. 153-182.
- POTTS, C.E. & WIEDER, B. (1972) : Precise time and frequency dissemination via the LORAN-C system. Institute of Electrical and Electronic Engineers, Proceedings, Vol. 60, No. 5, pp. 530-539.
- PRESSEY, B.G., ASHWELL, G.E. & FOWLER, C.S. (1956) : Change of phase with distance of a low-frequency ground wave propagated across a coastline. Institute of Electrical Engineers, Proceedings, No. 2082R, Vol. 103B, pp. 527-534.
- Radio Technical Commission for Marine Services (1981) : Minimum performance standards (MPS) for automatic coordinate conversion systems. Report of Radio Technical Commission for Marine Services Special Committee No. 75, RTCM Paper 378-81/DO-10.
- RAZIN, S. (1967) : Explicit (non iterative) Loran solution. *Navigation, Journal of the Institute of Navigation*, Vol. 11, No. 3, pp. 265-269.
- ROKITYANSKY, I.I. (1982) : Geoelectromagnetic investigation of the earth's crust and mantle. New York, Springer-Verlag, 1-381.
- SAMADDAR, S.N. (1979) : The theory of Loran-C ground wave propagation — a review. *Navigation, Journal of the Institute of Navigation*, Vol. 26, No. 2, pp. 173-187.
- SAMADDAR, S.N. (1980) : Weather effect on Loran-C propagation. *Navigation, Journal of the Institute of Navigation*, Vol. 27, No. 1, pp. 39-53.
- SANDERS, J.H. (1965) : The velocity of light. Pergamon Press, 141 p.
- SODANO, E.M. (1965) : General non iterative solution of the inverse and direct geodetic problems. *Bulletin Géodésique, nouvelle série*, n° 75.
- SMITH, E.K., Jr. & WEINTRAUB, S. (1953) : The constants in the equation for atmospheric refractive index at radio frequencies. Institute of Radio Engineers, Proceedings, Vol. 41, pp. 1035-1037.
- STANSELL, T.A. (1973) : Accuracy of geophysical offshore navigation systems. Torrance, Calif., Magnavox Advanced Products Division, Brochure No. MX-TR-2035-73.
- STANSELL, T.A. (1978) : The Transit navigation satellite system. Torrance, Calif., Magnavox Advanced Products Division, Brochure No. R-5933/Oct.
- STRATTON, J.A. (1941) : Electromagnetic theory. New York, McGraw Hill Book Company, 615 p.

- STUIFBERGEN, N. (1980) : Intersection of hyperbolae on the earth. Technical Report 77, University of New Brunswick, Canada.
- TERMAN, F.E. (1943) : Radio Engineer's Handbook. New York, McGraw Hill, 1-1019, section 10.
- THOMAS, P.D. (1970) : Spheroidal geodetics reference systems and local geometry. U.S. Naval Oceanographic Office, SP-138, Jan. (Now : Defense Mapping Agency, SPPUB-138).
- TORGE, W. (1980) : Geodesy. Translated from German by C. JEKELI. Berlin, Walter de Gruyter and Co., ISBN 3-11-007232-7.
- U.S. Coast Guard, Department of Transportation (1982) : Harbor monitor system quarterly status review for 1 Jan. 1982 through 31 March 1982. Groton, Connecticut, U.S. Coast Guard Research and Development Center.
- U.S. Coast Guard, Department of Transportation, 1980 to 1981. Radionavigation Bulletin, Washington, D.C., Nos. 1-9, June 1980 to June 1982.
- U.S. Coast Guard (G-WAN-2), Department of Transportation (1980) : Loran-C user handbook, Washington, D.C. Comdtinst M16562.3, pp. 1-82.
- U.S. Coast Guard (G-NRN-1), Department of Transportation (1981) : Specification of the transmitted Loran-C signal, Washington, D.C., Comdtinst M16562.4, July.
- Van der POL, B. & BREMMER, H. (1937, 1938, 1939) : The diffraction of electromagnetic waves from an electrical point source round a finitely conducting sphere. Philadelphia Magazine, Series 7, Vol. 4, pp. 141-176, 825-864; Vol. 25, pp. 817-834; Vol. 26, pp. 261-275.
- WAIT, J.R. (1964) : Electromagnetic surface waves, Advances in Radio Research, New York, Academic Press, Vol. 1, pp. 157-217.
- WAIT, J.R. (1969) : Concerning the theory of scatter of HF radio ground waves from periodic sea waves. Boulder, Colorado, Electronic Probing in Geophysics, Golem Press, Appendix B, pp. 361-369.
- WAIT, J.R. (1971) : On the theory of radio propagation over a slightly roughened curved earth. Boulder, Colorado, Electronic Probing in Geophysics, Golem Press, Appendix C, pp. 370-381.
- WAIT, J.R. (1981) : Wave propagation theory. New York, Pergamon Press, 1-346.
- WAIT, J.R. (1982) : Geo-Electromagnetism. New York, Academic Press, 1-268.
- WARREN, R.S., GUPTA, R.R. & SHUBBUCK, T.J. (1978) : Design and calibration of a grid prediction algorithm for the St. Mary's River Loran-C chain. The Wild Goose Association, Annual Technical Symposium, 7th, Proceedings, pp. 134-143.
- WATSON, G.N. (1918) : The transmission of electric waves around the earth. The Royal Society, Proceedings, Vol. A95, pp. 546-563.
- WESEMAN, J.F. (1982 a) : Preliminary data from the Sept. 1981, New England Coast Calibration or Rate 9960 (private communication).
- WESEMAN, J.F. (1982 b) : Loran-C — Present and future. Navigation, Journal of the Institute of Navigation, Vol. 29, No. 1, pp. 7-21.
- WINKLER, G.M.R. (1972) : Path delay, its variations, and some implications for the field use of precise frequency standards. Institute of Electrical and Electronic Engineers, Proceedings, Vol. 60, No. 5, pp. 522-529.

APPENDIX A

The arc-length tables and code shown in UIB-82 give :

1. Arc-length differences versus range and azimuth for the SODANO (1965), COLLINS (1980), and LAMBERT (1942) methods, using computer software with 7, 8-9 and 11 significant digit precision.
2. Program "check-out" examples giving distance, azimuth and time computed by the SODANO (1965) and DMA (RTCM, 1981) methods.
3. Station coordinates used for the tables in 2A.
4. Double precision Fortran subroutine of the SODANO (1965) arc-length method used in computations of Tables 1A and 2A.

SODANO (1965) proved least sensitive to computer precision as shown in Tables 1A, 2A and 3A. The data shown were generated by the HP-1000 RTE IV double precision ($\pm 2^{39} - 1$, i.e. 11-12 places), the HP-1000 RTE IV single precision ($\pm 2^{24} - 1$, i.e. 7 places) and an Apple II⁺ computer (8-9 places). As seen in Table 1A (column 3), both COLLINS and SODANO agree within ± 1 meter. COLLINS (1980) shows much greater differences (column 5) at short distances with the lower (7 places) precision. Conversely, LAMBERT (1942) has the larger differences with higher precision (column 4) and greater differences at all distances (column 6) with the lower precision (7 places). Additionally, checks were run against examples given by THOMAS (1970) on the Apple II⁺ and agreed within ± 0.5 meters at distances of 8,466 and 10,102 km. The results are in general agreement with the recent work of APL (1982).